



Spatial distribution of hydrogen sulfide and sulfur species in coastal marine sediments Hiroshima Bay, Japan

Asaoka, Satoshi ; Umehara, Akira ; Otani, Sosuke ; Fujii, Naoki ;
Okuda, Tetsuji ; Nakai, Satoshi ; Nishijima, Wataru ; Takeuchi, Koji ;...

(Citation)

Marine Pollution Bulletin, 133:891-899

(Issue Date)

2018-08

(Resource Type)

journal article

(Version)

Accepted Manuscript

(Rights)

© 2018 Elsevier.

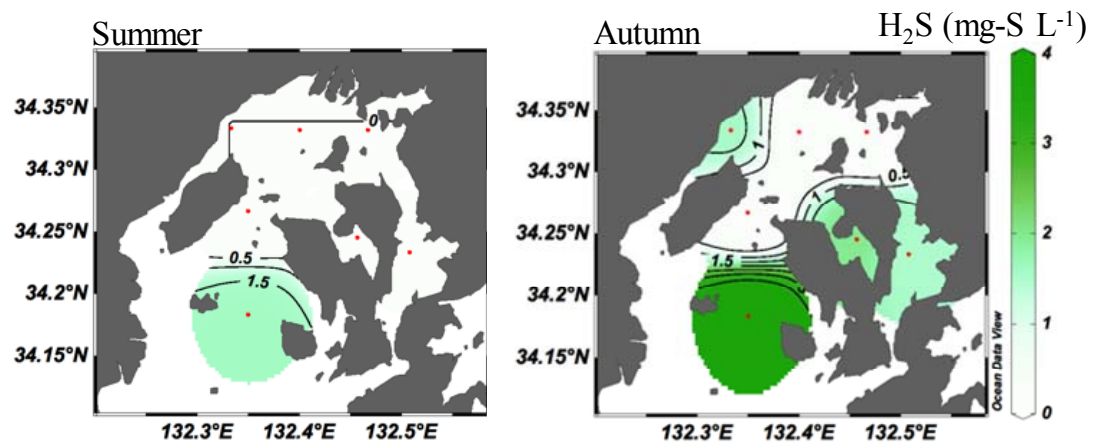
This manuscript version is made available under the CC-BY-NC-ND 4.0 license
<http://creativecommons.org/licenses/by-nc-nd/4.0/>

(URL)

<https://hdl.handle.net/20.500.14094/90004983>



Graphical abstract



The spatial distributions of hydrogen sulfide concentration in surface sediments pore water in Hiroshima Bay, Japan

Highlights

- Sulfur species in marine sediments in Hiroshima Bay, Japan was investigated.
- We used detection tubes and X ray absorption fine structure methods.
- The H_2S in sediment pore water ranged <0.1 to 4 mg-S L^{-1} .
- The sulfur species were identified as sulfate, thiosulfate, sulfur and pyrite.
- Formation of pyrite and sulfur played an important role on scavenging H_2S .

1 Spatial distribution of hydrogen sulfide and sulfur species in coastal marine sediments

2 Hiroshima Bay, Japan

3
4 Satoshi ASAOKA^{a*}, Akira UMEHARA^b, Sosuke OTANI^c,

5 Naoki FUJII^d, Tetsuji OKUDA^e, Satoshi NAKAI^f, Wataru NISHIJIMA^b,

6 Koji TAKEUCHI^g, Hiroshi SHIBATA^g, Waqar Azeem JADOON^a, Shinjiro

7 HAYAKAWA^f

8
9 ^aResearch Center for Inland Seas, Kobe University

10 5-1-1 Fukaeminami, Higashinada, Kobe, 658-0022 JAPAN

11 ^bEnvironmental Research and Management Center, Hiroshima University

12 1-5-3, Kagamiyama, Higashihiroshima, Hiroshima, 739-8513 JAPAN

13 ^cDepartment of Technological Systems, Osaka Prefecture University College of

14 Technology

15 26-12, Saiwaicho, Neyagawa, Osaka, 572-8572 JAPAN

16 ^dInstitute of Lowland and Marine Research, Saga University

17 1, Honjyo, Saga, 840-8502 JAPAN

18 ^eFaculty of Science & Technology, Ryukoku University

19 1-5 Yokotani, Setaooe, Ootsu, Shiga 520-2194, JAPAN

20 ^fGraduate School of Engineering, Hiroshima University

21 1-4-1 Kagamiyama, Higashi-Hiroshima, Hiroshima 739-8527, JAPAN

22 ^gNational Institute of Technology, Hiroshima College

23 4272-1, Higashino, Oosakikamishima, Toyota, Hiroshima 725-0231, JAPAN

24

25 *Corresponding author:

26 Tel & Fax: +81-78-431-6357, E-mail: s-asaoka@maritime.kobe-u.ac.jp

27 Address: Research Center for Inland Seas, Kobe University, 5-1-1 Fukaeminami,

28 Higashinada, Kobe, 658-0022 JAPAN

29

30

31

32

33

34

35

36

Abstract

This study aims to reveal spatial distribution of hydrogen sulfide and sulfur species in marine sediments in Hiroshima Bay, Japan, by direct analyses using a combination of detection tubes and X-ray absorption fine structure spectroscopy. In summer and autumn, the hydrogen sulfide concentration ranged from <0.1 to 4 mg-S L^{-1} . In this study, only hydrogen sulfide was observed in autumn and at two stations in summer. In contrast, some earlier studies reported in all seasons in Hiroshima Bay the presence of acid volatile sulfide, which is used as a proxy of sulfide content. The sulfur species in sediments were mainly identified as sulfate, thiosulfate, elemental sulfur, and pyrite. Thiosulfate was a minor component compared to the other sulfur species. The formation of pyrite and sulfur derived from hydrogen sulfide oxidation played an important role in the scavenging of hydrogen sulfide.

Key Words

Detection tube, Eutrophication, Pyrite, Sediment, Sulfur cycle, X-ray absorption fine structure

55 **1. Introduction**

56 In enclosed water bodies such as inland seas, ports, and harbors, coastal marine
57 sediments are affected by significant terrigenous organic matter loads. Thus, the high flux
58 of organic matter leads to the rapid depletion of oxygen in the sediments due to intense
59 microbial activity. Under such anoxic conditions, sulfate-reducing bacteria (SRB) utilize
60 sulfate as a terminal electron acceptor for the degradation of organic matter and generates
61 hydrogen sulfide (Muyzer and Stams, 2008). Hydrogen sulfide can also cause blue tide
62 called 'Aoshio' (Otsubo et al., 1991), which is the formation of colloidal sulfur derived
63 from the upwelling of hydrogen sulfide with anoxic bottom waters. This process
64 consumes dissolved oxygen in the water column and gives off a bad odor. Approximately
65 27-50% of oxygen demand was oxidation of reduced species such as Mn(II), Fe(II), H₂S
66 in Hiroshima Bay (Seiki et al., 1994; Yamamoto et al., 2011). Therefore, hydrogen sulfide
67 is a significant contributor to the development of hypoxia. Additionally, hydrogen sulfide
68 can cause serious problems for fisheries and benthic ecosystems because it is highly
69 reactive and toxic. The toxicity of hydrogen sulfide for plants and aquatic organisms
70 results from hydrogen sulfide interfering with cytochrome c oxidase, the last enzyme of
71 the electron transport system (Raven and Scrimgeour, 1997; Gray et al., 2002; Affonso et
72 al., 2004; Lloyd, 2006; Dooley et al., 2013). Most aquatic organisms are negatively

affected by hydrogen sulfide in the range of 0.094-1.9 mg-S L⁻¹ (Marumo and Yokota, 2012). Therefore, hydrogen sulfide has been generally detected and found to be a threat for benthic ecosystems in enclosed and/or semi-enclosed water bodies (Wang and Chapman, 1999; Caddy, 2000; Sakai et al., 2013; Yamamoto et al., 2015).

The sulfide contents including hydrogen sulfide in marine sediments have been conventionally evaluated by measuring acid volatile sulfide (AVS). This is a simple method by which hydrogen sulfide gas is released from sediments by the addition of acid (Rickard and Morse, 2005). Therefore, AVS is widely used in the fields of biogeochemistry, environmental science, and fisheries sciences (Jonge et al., 2010; Machado et al., 2010; Simpson et al., 2012; Gao et al., 2013; Arfaeinia et al., 2016). However, AVS is operationally defined as a component of sedimentary sulfide (from both pore water and sediment) and potentially includes dissolved sulfur species, FeS clusters, iron sulfide nanoparticles, mackinawite (FeS), greigite (Fe₃S₄), and pyrite (FeS₂; Rickard and Morse, 2005). Therefore, AVS may exaggerate the hydrogen sulfide concentration and may detect hydrogen sulfide even if it is not present in the sediments (**Fig. S1**). In the case of sediments, sequential extraction is conventionally used to specify sulfur species (Nriagu and Soon, 1985; Rice et al., 1993; Thamdrup et al., 1994). In spite of their widespread use, there are concerns that sequential extractions might give misleading

results because the method is complicated and time-consuming. For example, sequential extraction bears a high risk of misinterpretation due to the redistribution, readsorption, and oxidation of the analyte during the sequential extraction steps (Calmano, et al., 2001). Therefore, it might not be appropriate to use sequential extraction to identify the sulfur species in marine sediments (**Fig. S1**). However, precisely identifying chemical species of sulfur in marine sediment is imperative for revealing the reductive and oxidative pathways of the sulfur cycle as well as the degradation of organic matter (Jørgensen and Kasten, 2006; Muyzer and Stams, 2008; Risgaard-Petersen et al., 2012, Pjevac et al., 2014; Markovic et al., 2015). To reliably determine the concentration of highly reactive and unstable hydrogen sulfide, rapid and on-site measurements were required. Previously, many methods such as spectrophotometric detection including the methylene blue method, the flow injection method, fluorimetric detection including a hydrogen sulfide sensor, 2-D hydrogen sulfide measurement, chemical probes, and gas chromatography were used to determine the hydrogen sulfide concentration (Cline, 1969; Kubán et al., 1992; Radford and Cutter, 1993; Lawrence et al., 2000; Choi and Hawkins, 2003; Zhu and Aller, 2013; Li et al, 2013; Zhang and Guo, 2014). However, these methods are not always appropriate for on-site and rapid analyses. The concentrations of hydrogen sulfide in sediments were investigated in a hypersaline lake, a lagoon (Habicht and Canfield, 1997), brackish water

basins (Scholz et al, 2013), brackish water bodies (Jørgensen, 1977), a coastal brackish lake (Sakai et al., 2013) and a eutrophic saline lake (Reese et al., 2008). However, field observations involving the direct determination of hydrogen sulfide in enclosed water bodies, especially those located adjacent to densely populated areas, are limited.

In this study, to overcome these problems, we used a detection tube and X-ray absorption fine structure (XAFS) spectroscopy. The detection tube can measure the concentration of hydrogen sulfide in sediment pore water on-site. This simplified and rapid determination method (ca. 3 min) accurately measured the concentration of hydrogen sulfide without oxidation loss of hydrogen sulfide. XAFS has been used to identify chemical species with minor or no pretreatments, and thus it offers a great advantage over conventional sequential extraction methods by keeping the sulfur species in marine sediments. XAFS can determine redox status and coordination environment for a wide variety of elements, including sulfur, carbon and nitrogen within these sediments. XAFS has been applied to the analysis of the chemical form and oxidation state of sulfur in soil and sediments (Bostic et al, 2005; Jalilehvand, 2006; Burton et al, 2009). Additionally, the collected sediments were immediately stored at 4°C in vacuum bags to seize/minimize all biological, physical, and chemical activities. The purpose of this study was to reveal the spatial distribution of hydrogen sulfide and sulfur species in coastal

marine sediments in Hiroshima Bay, Japan using a combination of the detection tube method and XAFS spectroscopy (**Fig. S1**).

2. Experimental

2.1 Study site

Seawater and sediment samples were collected from seven stations in northern Hiroshima Bay, Japan on 2-3 November 2014 (Autumn cruise), 7 February 2015 (Winter cruise), 9 May 2015 (Spring cruise) and 20 August 2015 (Summer cruise) by a training and research vessel, HIKARI, of the National Institute of Technology, Hiroshima College (**Fig. 1**). The coordinates of the sampling sites are shown in **Table S1**. Hiroshima Bay is situated in the Seto Inland Sea, Japan. The enclosed bay is about 30 km from east to west and 50 km from north to south, with a total area of 1043 km² and an average depth of 26 m. The bay is significantly affected by intensive oyster culturing (annual production approximately 19,000 tons on an oyster meat basis) and terrigenous loads from the Ota River (catchment area: 1710 km²; average river water discharge: 7.14 x 10⁶ m³ d⁻¹; Yamamoto et al., 2002). Station 1 is located near the industrial zone and is affected by domestic and industrial wastewater. Stations 2-4 are situated in the northern part of Hiroshima Bay and are adjacent to a big metropolitan area, Hiroshima city. The

terrigenous loads from the Ota River form halocline in the northern part of Hiroshima Bay every summer. Stations 5 and 6 are located in the western part of Hiroshima Bay and were affected by seawater intrusion from the southern part of Hiroshima Bay. Station 7 is located inside the enclosed bay called Etajima Bay where intensive oyster culture is conducted.

2.2 Analytical parameters

Vertical profiles of temperature, salinity and dissolved oxygen concentration were measured using a multi probe (AAQ176; JFE Advantec).

Surface sediments were collected at seven stations in the spring, summer and winter using an Ekman-Birge bottom sampler (20 cm x 20 cm; Rigo). In autumn, sediment core samples were collected using an undisturbed core sampler (ø11 cm, 50 cm long; HR type; Rigo) at Sts. 1, 3, 5, 6 and 7. Whereas, at Sts. 2 and 4, the Ekman-Birge bottom sampler was used to collect surface sediments because we could not deploy the undisturbed core sampler due to a strong wind. The collected cores were cut at every 5 cm on board. The surface sediments collected by the Ekman-Birge bottom sampler were taken from the top layer (5 cm). On board, these sediments were immediately transferred into vacuum packs, the air was removed to prevent oxidation and then the packs stored in a refrigerator at 4°C

until they could be transferred to the laboratory. Successively, the sediments were vacuum-dried at 45°C and ground using an agate-made mortar. The homogenized sediments were stored in vacuum packs to maintain the chemical states of sulfur for XAFS analyses.

The sediment pore water was collected by the rhizon method using a soil moisture sampler that consisted of a syringe and a 50-mm long and ϕ 2.5-mm fiber filter (DIK-305A; Daiki Rika Kogyo). This soil moisture sampler has several advantages when compared with other sampling devices: low mechanical disturbance of the sediment due to the small diameter of 2.5 mm and the absence of direct contact with atmospheric oxygen resulting in minimal loss/oxidation of hydrogen sulfide. The fiber filter was installed in the sediments to suck out a few mL of sediment pore water. The on-site concentration of hydrogen sulfide in the pore water was measured by inserting a detection tube (detection limit: 0.1 mg-S L⁻¹) within 3 min (200SB: Komyo Rikagaku Kogyo).

The formation of a brown-colored PbS band in the detection tube due to the reaction of hydrogen sulfide and lead is the indicator that hydrogen sulfide is present in the pore water. The length of the brown-colored PbS band in a detection tube is correlated with hydrogen sulfide concentration. The oxidation rate constant of our proposed method ranged from 0.0069-0.0151 min⁻¹ (Asaoka et al., 2012a). Considering this oxidation rate

and the range of observed hydrogen sulfide concentrations, the loss of hydrogen sulfide by oxidation through this procedure was estimated at less than 5%.

The oxidation and reduction potential (Eh) and pH of the sediments were measured using Eh and pH electrodes (RM-30P; DKK-TOA, C-62; AS ONE). The total organic carbon (TOC), total nitrogen (TN), and total sulfur (TS) of the sediments were determined by an elemental analyzer (CHNS/O 2400II; Perkin Elmer). The sediment samples were acidified to remove carbonate before TOC, TN, and TS analyses were performed according to the method of Yamamuro and Kayanne, 1995.

For carbon and nitrogen isotope analyses, terrigenous particulate organic matter (POM) and leaves collected from the upstream (34°-30.0'N; 132° -30.7'E) and middle stream (34° -26.3'N; 132° -28.9'E) of the Ota river, marine POM collected from Hiroshima Bay (34° -11.0'N; 132° -21.0'E; St.6), and benthic micro algae grown in the Jigozen tidal flat located in the innermost part of Hiroshima Bay (34° -20.1'N; 132° -19.3'E) were used. Carbon and nitrogen isotopes corresponding to $\delta^{13}\text{C}$ and $\delta^{15}\text{N}$ for seawater and river water, sediment, and terrestrial plant samples were measured using the following procedure. The GF/F filter (seawater and river water), sediment, and terrestrial plant samples were treated with 1 mol L⁻¹ HCl to remove inorganic carbonates, and $\delta^{13}\text{C}$ and $\delta^{15}\text{N}$ of the POM were analyzed by an elemental analyzer-isotope ratio mass

spectrometer (FlashA EA1112-DELTA V ADVANTAGE, Thermo Fisher Scientific, MA, USA). The isotope ratios are expressed in delta notation (‰) in Equation 1.

$$\delta^{13}\text{C} \text{ or } \delta^{15}\text{N} (\text{‰}) = \left(\frac{R_{\text{sample}}}{R_{\text{standard}}} - 1 \right) \times 10^3 \quad (1)$$

where R is the $^{13}\text{C}/^{12}\text{C}$ or $^{15}\text{N}/^{14}\text{N}$ ratio for $\delta^{13}\text{C}$ or $\delta^{15}\text{N}$, respectively. Pee Dee Belemnite (PDB) and air N_2 were used as references for $\delta^{13}\text{C}$ and $\delta^{15}\text{N}$, respectively.

XAFS analyses of the sulfur K-edge spectra (range 2460-2490 eV; step size 0.2 eV) were performed using the BL11 at the Hiroshima Synchrotron Research Center (HiSOR) (Asaoka et al, 2012b). The synchrotron radiation from a bending magnet was monochromatized with a Si(111) double-crystal monochromator. The XAFS spectra of the sediment samples were measured using X-ray fluorescence yield mode with a SDD detector (XR-100SDD; AMPTEK) under a He gas environment. The K-edge main peak of sulfate derived from $\text{CuSO}_4 \cdot 5\text{H}_2\text{O}$ was calibrated to 2481.6 eV. The sediment samples were mounted on double-stick tape (NW-K15; Nichiban) and placed in the central hole (15-mm diameter) of a copper plate. The angle between the incident X-ray and the sample surface was adjusted to 20° , and the X-ray fluorescence was detected from the direction normal to the incident beam in the plane of the electron orbit of the storage

ring. The standards $\text{FeSO}_4 \cdot 7\text{H}_2\text{O}$ (Wako Pure Chemical Industry), Na_2SO_3 (Wako Pure Chemical Industry), $\text{Na}_2\text{S}_2\text{O}_3$ (Wako Pure Chemical Industry), elemental sulfur (Wako Pure Chemical Industry) and FeS_2 (Stream Chemicals), FeS (Wako Pure Chemical Industry), MnS (Sigma-Aldrich) and L-Cysteine (Wako Pure Chemical Industry) representing sulfate, sulfite, thiosulfate, sulfur, pyrite, iron sulfide, manganese sulfide and cysteine, respectively, were also measured using both the conversion electron yield mode and the X-ray fluorescence yield mode simultaneously. XAFS analyses were carried out using XAFS spectra processing software (REX2000 ver. 2.6: Rigaku Co. Ltd.). The quantification error associated with linear combination fitting is approximately 5% for each sulfur species (Burton et al., 2009).

The contour maps of hydrogen sulfide and sulfur species in sediments were drawn using software for the analysis and visualization of oceanographic and meteorological data sets (Ocean Data View ver 4.7.10 ; Schlitzer, 2017).

The Eh-pH diagram for the Fe-S- H_2O system was calculated using the thermodynamic simulation software Geochemist's Workbench 8 (RockWare). In this calculation, HCO_3^- activity was set at 0.002, which was the actual HCO_3^- concentration considering the CO_2 gas pressure. The activities of Na^+ , K^+ , Mg^{2+} , Ca^{2+} , Cl^- and SO_4^{2-} in seawater were calculated, followed by the activity coefficients (Whitfield, 1973). The total dissolved

Fe(II) activity was set to be 10^{-9} (Rickard and Luther, 2007). The pressure and temperature were set at 1.013 hPa and 25 °C, respectively.

3. Results

3.1 Hydrogen sulfide concentration in the sediment pore water

The spatial distributions of hydrogen sulfide in the surface sediment (0-5 cm depth) pore water collected from Hiroshima Bay, Japan are shown in **Fig. 2**. Based on the distribution of hydrogen sulfide in the surface sediment pore water, clear seasonal variations were observed. In the spring and winter, hydrogen sulfide was not detected ($< 0.1 \text{ mg-S L}^{-1}$) in the surface sediment pore water. In the summer, the concentrations of hydrogen sulfide in the surface sediment pore water at Sts. 6 and 7 were 1.6 and 0.2 mg-S L^{-1} , respectively (**Fig. 2**). At the other stations, the hydrogen sulfide concentrations were below the detection limit ($< 0.1 \text{ mg-S L}^{-1}$).

In the autumn, the hydrogen sulfide concentrations in the surface sediment pore water at Sts. 1, 4, 6, and 7 were 1.5, 1.6, 4, and 2 mg-S L^{-1} , respectively. The vertical profiles of the hydrogen sulfide concentration in the core sediment pore water are shown in **Fig. 3**. Generally, the concentrations of hydrogen sulfide in the sediment pore water at depths of 7.5 cm and below were higher than that of pore water from the surface layer. For example,

the concentration of hydrogen sulfide in the surface layer at Sts. 1, 6, and 7 were 1.5, 4, and 2 mg-S L⁻¹, while, at depths of 7.5 cm and below the concentrations were 6-10, 6-9, and 10-28 mg-S L⁻¹, respectively.

3.2 Sulfur species of the surface sediments

Pyrite (FeS₂) and iron monosulfide (FeS) play a central role in the sulfur and iron cycles of marine sediments (Schippers and Jørgensen, 2002). Sulfur species in the surface sediments in this study fit well with the combination of sulfate, thiosulfate, elemental sulfur, and pyrite by the linear combination fit. In contrast, the XAFS spectra of iron sulfide was not observed because iron sulfide was oxidized by MnO₂ in marine sediments (Aller and Rude, 1988). The XAFS spectra of sulfite, manganese sulfide, cysteine and other sulfur species were not observed, either. Hence, these sulfur species were considered minor components in the sediments. Therefore, these minor components of sulfur species were not used by the linear combination fit to minimize overfitting attributed to increasing number of latent variables (Kuno et al., 1999). The example of the linear combination fit of sulfur species at St. 1 is shown in **Fig. S2**. The concentrations of sulfur species on a dry basis were calculated using the TS content obtained by the elemental analyzer and the composition of sulfur species determined by XAFS (**Fig. 4 and Table S2**). The sulfate

271 concentration of surface sediment was in the range of 0.5-6.9 mg-S g⁻¹. The sulfate
272 showed the same spatial distributions from autumn to spring and had a peak of 3.7-6.9
273 mg-S g⁻¹ at St. 4. In summer, the sulfate was more or less equally distributed in the
274 northern and eastern parts of the bay. The lowest (0.5 mg-S g⁻¹) concentration of sulfate
275 in summer was observed at St. 5. Thiosulfate (0-2.1 mg-S g⁻¹) was a minor component
276 compared to the other sulfur species reported in all of the seasons (**Fig. 4**). The
277 concentration of elemental sulfur in the surface sediment showed seasonal variations. The
278 elemental sulfur concentration had a peak of 1.6 mg-S g⁻¹ at St.7 in autumn. In winter, the
279 sulfur was almost uniformly distributed in the range of 1.0-1.4 mg-S g⁻¹. Thereafter, in
280 spring, the elemental sulfur concentration showed peaks of 2.2 and 2.8 mg-S g⁻¹ at Sts. 4
281 and 7, respectively. In summer, elemental sulfur peaks of 2.3 and 2.7 mg-S g⁻¹ were
282 observed at Sts. 2 and 4, respectively. The pyrite concentrations in the surface sediments
283 also showed seasonal variations. In autumn, the pyrite concentrations at St. 1 and in the
284 northern part of the bay (Sts. 2, 3 and 7) were 0.7-2.7 mg-S g⁻¹. In contrast, at the other
285 stations, pyrite was not identified. In winter and spring, the pyrite concentration in the
286 eastern part of the bay was high compared to the other areas of Hiroshima Bay. In summer,
287 significant pyrite peaks were observed at stations 1 (2.0 mg-S g⁻¹), 3 (3.4 mg-S g⁻¹), and
288 7(3.8 mg-S g⁻¹), respectively.

289

290 ***3.3 Dissolved oxygen concentration of bottom water***

291 The dissolved oxygen concentrations of bottom water (1 m above the seabed) at the
292 seven stations ranged from 7.4 to 8.5 mg L⁻¹, 1.4 to 5.4 mg L⁻¹, 6.0 to 7.0 mg L⁻¹ and 8.2
293 to 8.9 mg L⁻¹ in spring, summer, autumn, and winter, respectively (**Fig. 5**). In summer,
294 the bottom water was observed to have poor oxygen water mass at St. 1, in the northern
295 part of the bay (Sts. 2-4), and at St. 7. The concentrations of dissolved oxygen at St. 1,
296 Sts. 2-4, and St. 7 in summer were 1.4, 1.7-3.5, and 4.1 mg L⁻¹, respectively.

297

298 ***3.4 Physico-chemical characteristics of surface sediments***

299 This study also investigated Eh, TOC, TON and C/N_{org} of the surface sediments (**Table**
300 **1**). The Eh of surface sediments at the seven stations ranged from -55 to 112 mV, -139 to
301 28 mV, -129 to -50 mV, and -45 to 130 mV in spring, summer, autumn, and winter,
302 respectively (**Table 1**). In summer and autumn, the lowest Eh values were observed. In
303 contrast, the pH levels of surface sediments did not show seasonal variations and ranged
304 from 7.7 to 8.6 (**Table 1**).

305 The annual averages of the TOC, TON, and C/N_{org} ratios of surface sediment are given
306 in **Table 2**. The concentrations of the TOC, TON, and C/N_{org} ratios in surface sediments

ranged from 2.0 to 2.7%, 0.22 to 0.32%, and 8.5 to 9.2, respectively. The loss on ignition (LOI), COD of sediments and mud content near the 7 stations were also shown in **Table 2** (Hibino and Matsumoto, 2006; monitoring data by the Ministry of Land, Infrastructure, Transport and Tourism, Japan). The LOI, COD of sediments and mud content ranged 9.9 to 12%, 37 to 57 mg g⁻¹ and 10.3 to 74.7%, respectively.

4. Discussion

The hydrogen sulfide distribution is controlled by biogenic and abiogenic reactions such as sulfide oxidation, sulfate reduction, metal sulfide precipitation and dissolution, nucleophilic additions to organic matter, and acid base equilibria (Morse et al, 1987; Schippers and Jørgensen, 2002; Jørgensen and Kasten, 2006; Zhu and Aller, 2013). The biogenic reactions involve hydrogen sulfide formation through sulfate reduction by SRB under anoxic conditions and bacterial oxidation of hydrogen sulfide to sulfate via sulfur with phototrophic or chemotrophic sulfur bacteria under anoxic or oxidizing conditions, respectively (Gemerden, 1993). The abiogenic reactions, which are chemical processes, include the formation of colloidal sulfur and sedimentary pyrite (Otsubo et al., 1991). The dissolved oxygen concentration of the bottom water is contributory to a change in the concentration of hydrogen sulfide because the dissolved oxygen serves as an oxidizer of

hydrogen sulfide. However, there is no significant relation between the hydrogen sulfide concentration in surface sediment pore water and the dissolved oxygen concentration of bottom water ($r=0.032$; **Fig. S3**). Even though the dissolved oxygen concentration of bottom water was over 4.1 mg L^{-1} , hydrogen sulfide was detected, suggesting that the sulfate reducing rate, namely, the hydrogen sulfide formation rate, was high compared to the hydrogen sulfide oxidation rate in the stations where the hydrogen sulfide was detected. Another possibility is high rates of oxygen uptake at the sediment surface. The dissolved oxygen concentration significantly decreased at diffusive boundary layer at 0.4-0.5 mm above the sediment-water interface (Jørgensen and Revsbech, 1985; Archer et al., 1989). Therefore, the sediment-water interface might become anoxic conditions which was sufficient for detecting hydrogen sulfide.

Sediment Eh is an effective indicator of redox sequence. The sulfate reduction rate of SRB is well related with Eh. The sulfide production rate significantly increases around $\text{Eh} < \text{ca. } -100 \text{ mV}$ (Hata, 1960). However, SRB can use nitrate or even oxygen as an electron acceptor under oxidizing conditions (McCready et al., 1983; Dilling and Cypionka, 1990), indicating that sulfate reduction was conducted by SRB throughout the seasons. These previous reports are supported by this study as well. The hydrogen sulfide concentration of the sediment pore water significantly increased at Eh levels below -84

mV (**Fig. 6**). In winter and spring, the sediment Eh ranged from -45 to +130 mV and -55 to +112 mV, respectively. These high Eh values occurred due to the high dissolved oxygen concentrations of the overlying water (1 m above the sea bottom) in the winter (8.2-8.9 mg L⁻¹; **Fig. 5**) and spring (7.4-8.5 mg L⁻¹; **Fig. 5**). The surfaces of the sediments in winter and spring were under aerobic conditions, indicating that the sulfate reduction rate by SRB which was strictly anaerobic bacteria might decrease under aerobic conditions. Hence, the oxidation rate of hydrogen sulfide was considered to exceed the sulfate reduction rate of SRB.

In summer, a poor oxygen water mass was observed in overlying water at Sts. 1-4 (1.4-3.5 mg L⁻¹) and St. 7 (4.1 mg L⁻¹; **Fig. 5**). Both haloclines and thermoclines were observed at all stations in summer (**Figs. S4a and S4b**), which could have obstructed the supply of oxygen to the bottom of the sea during summer, and dissolved oxygen in the overlying water was consumed by organic matter decomposition and by the oxidation of reduced substances.

The Eh level of the sediment was less than -100 mV except at Sts. 2 and 6, indicating that the conditions were sufficient for detecting hydrogen sulfide. However, hydrogen sulfide was detected at St. 6 (1.6 mg-S L⁻¹; **Fig. 2**). The COD which is utilized as electron donors by sulfate reducing bacteria (Liamleam and Annachhatre, 2007) was highest at St.

6 (57 mg g^{-1}) compared to other stations (37 to 49 mg g^{-1} ; **Table 2**). The COD of the sediments in Hiroshima Bay was mainly derived from inner production and decomposed easily (Hibino et al., 2006). Therefore, the sediment at St. 6 is more favorable to reduce sulfate to hydrogen sulfide by SRB compared to other stations. In the case of other stations, the peaks and high concentrations of pyrite at Sts. 1, 3, and 7 and of elemental sulfur at Sts. 2 and 4 confirm the removal of hydrogen sulfide (**Fig. 4b**). In most coastal sediments, less than 10% of the produced hydrogen sulfide is preserved as iron sulfide or pyrite, while the rest is oxidised or lost to the atmosphere (Jørgensen, 1987). Therefore, hydrogen sulfide might have been mainly scavenged by the formation of pyrite at Sts. 1, 3, and 7 under reduced condition which could be supposed by low Eh '(-115 to -102 mV). At Sts. 2 and 4, hydrogen sulfide might have been mainly oxidized to elemental sulfur because Eh of the sediments at St. 2 was 15 mV, or not extremely reduced condition compared to other stations (**Table 1**). Although the Eh of the sediments at St. 4 was -130 mV, DO of overlying water was not depleted (3.5 mg L^{-1} ; **Fig. 5**). Hence, hydrogen sulfide at St 4 might have been oxidized, resulting the lack of detection of hydrogen sulfide at these stations. Hence, hydrogen sulfide was detected at St. 6 because it was not scavenged well through the formation of pyrite or elemental sulfur.

In autumn, although haloclines were slightly observed at Sts. 3 and 4 due to fresh water

inflow from the Ota river, the vertical mixing of seawater resulted in the disappearance of haloclines at Sts. 1, 2, 5, 6, and 7 (**Figs. S4c and S4d**). Therefore, the dissolved oxygen concentrations of the overlying water were 6.0-7.0 mg L⁻¹ (**Fig. 5**). However, hydrogen sulfide was observed at Sts. 1, 4, 6 and 7. The COD of sediments which is electron donors of the sulfate reducing ranged 42 to 57 mg g⁻¹ and was higher than that of other stations (**Table 2**). In Hiroshima Bay, the apparent settling velocities of particulate matter that mainly originated from primary production become highest in October in correspondence with the beginning of vertical mixing (Seiki et al., 1985). The weight ratio of TOC to total organic nitrogen (C/N_{org.} ratio) is one of the indices used to distinguish between planktonic and terrestrial sources of organic matter (Sampei and Matsumoto, 2001). The C/N_{org.} ratios of all sampling stations ranged from 8.5 to 9.2, indicating that organic matter in sediments mainly originates from plankton (**Table 2**). Carbon ($\delta^{13}\text{C}$) and nitrogen ($\delta^{15}\text{N}$) isotopes of the sediments were also measured. A mixing model utilizing $\delta^{13}\text{C}$, $\delta^{15}\text{N}$, and three endmembers was used to identify the source of organic matter in the sediments (Phillips, 2012). The three endmembers used in this study were (1) terrigenous POM, (2) marine POM, and (3) benthic micro algae. The annual average contribution of terrigenous POM sources to organic matter in sediments was 21.8 to 29.8%, with the other sources being marine POM and benthic micro algae

(**Fig. 7 and Fig. S5**). Therefore, marine POM and benthic micro algae might be major contributors to the increase of sediment oxygen demand (SOD) because the labile fraction of POM derived from planktons in Hiroshima Bay was 70-80%, and it took from one to two months to decompose completely (Seiki et al., 1991). Hence, the high sedimentation flux of the POM from plankton in autumn might trigger an increase in SOD to decompose the POM and lead to depletion of DO at the sediment-water interface (Jørgensen and Revsbech, 1985; Archer et al., 1989) and the formation of hydrogen sulfide. St. 6 showed the highest concentration of hydrogen sulfide in the sediment pore water of all of the stations. The sedimentation rate of the bay was highest at the river mouth of the Ota River, in the innermost area of the bay (near Sts. 3 and 4; 0.60-0.68 g cm⁻²). The peak of the sedimentation rate was also observed around St. 6 (0.41 g cm⁻²) due to the presence of the center of counter clock-wise current transferring and depositing particle matter derived from the northern parts of Hiroshima Bay and inflowing rivers located at western parts of Hiroshima Bay (Hoshika, 2008). The COD and mud content of the sediments at St. 6 were 57 mg g⁻¹ and 74.3%, respectively and were highest or second highest of all the stations (**Table 2**). Therefore, the sediment at St. 6 is significantly affected by the sedimentation flux. Furthermore, pyrite formation is one of the factors that reduces the concentration of hydrogen sulfide in the sediment pore water. The Eh-pH diagram for the Fe-S-H₂O system

was calculated to clarify the pH and Eh conditions needed to form pyrite (**Fig. 8**). The sediment Eh and pH levels at St. 6 in autumn were -84 mV and 7.8, respectively, which were thermodynamically out of range for forming pyrite, which results consisted with the Eh-pH diagram for the Fe-S-H₂O system (Wei and Osseo-Asare, 1996; Rickard and Luther, 2007). The pyrite concentration of the sediment at St. 6 in autumn was relatively low (0.41 mg g⁻¹, **Fig. 4c**). Hence, hydrogen sulfide in the sediment pore water was not scavenged by the formation of pyrite. The major pathways of pyrite formation and pyrite oxidation are $\text{H}_2\text{S} \rightarrow \text{FeS} \rightarrow \text{FeS}_2$ and $\text{FeS}_2 \rightarrow \text{S}_2\text{O}_3^{2-} \rightarrow \text{S}_x\text{O}_6^{2-} \rightarrow \text{SO}_4^{2-}$, respectively (Rickard and Luther, 2007). We roughly estimated which reaction, pyrite formation or pyrite oxidation, was dominant using the sulfur composition of surface sediments. The sulfate and thiosulfate composition of sediments correlated with those of pyrite ($r=0.877$; **Fig. 9**). At St.6, sulfate and thiosulfate were major components of the sulfur species of the sediments from summer to winter, indicating that pyrite oxidation tended to be dominant from summer to winter. In contrast, pyrite formation tended to be dominant at Sts.1 and 3.

The age of the sediment core at St. 6 was roughly estimated using the sedimentation rate. The sediments at a depth of 22.5 cm originated in 1990. The vertical profile of hydrogen sulfide at St. 6 (**Fig. 3**) showed hydrogen sulfide at all depths. Therefore,

hydrogen sulfide might be observed steadily at St. 6 from summer to autumn. Similarly, a high hydrogen sulfide level was also observed at St. 7 due to the organic matter load from intensive oyster culturing (**Fig. 3**). At St. 7, the concentration of hydrogen sulfide in sediment pore water was high at depths of 7.5 cm and below (10-28 mg-S L⁻¹) compared to the surface layer (2.0 mg-S L⁻¹; **Fig. 3**), indicating that the hydrogen sulfide concentration gradient between the surface layer and depths of 7.5 cm and below was high. The hydrogen sulfide diffusion flux from the layer at a depth of 7.5 cm to the surface layer (2.5 cm) was roughly estimated based on Fick's laws of diffusion. The molecular diffusion coefficient of HS⁻ used in this calculation was 1.73 x 10⁻⁹ m² s⁻¹ based on Li and Gregory, 1974. The hydrogen sulfide diffusion flux from the layer at a depth of 7.5 cm to the surface layer was estimated to be 19 nmol s⁻¹ at St. 7, while those at other stations were 1.1-5.2 nmol s⁻¹. The hydrogen sulfide diffusion flux at St. 7 was high compared to those at other stations. Hence, the concentration of hydrogen sulfide in surface sediment pore water at St. 7 was more significantly affected by the deep layer through diffusion compared to other stations.

Finally, the hydrogen sulfide concentration in sediment pore water presented in this study was compared with the AVS of sediments reported by previous studies. The AVS in the innermost area of Hiroshima Bay (near St. 2) was approximately 0.3-1.1 mg g⁻¹

(Yamamoto et al., 2008). Similarly, AVS was detected in all seasons at St. 1 and near St. 7, and these values ranged ca. 0.2-1.0 and 0.2-0.7 mg g⁻¹, respectively (Tsujino et al., 2000; Yamamoto et al., 2015). In contrast, in this study, hydrogen sulfide was detected in sediment pore water in autumn at St. 1 and St. 7. Also, at St. 2, hydrogen sulfide was not detected any seasons. This difference between the AVS and hydrogen sulfide in sediment pore water was attributed to the difference in the sulfur species detected by each protocol. The AVS includes not only hydrogen sulfide but also dissolved sulfur species, FeS clusters, iron sulfide nanoparticles, mackinawite, greigite, and pyrite (Rickard and Morse, 2005). These sulfur species might be partially volatilized and detected as AVS by the addition of acid. Hence, AVS is not appropriate for used as a proxy of hydrogen sulfide concentration in sediment pore water.

5. Conclusion

In Hiroshima Bay, seasonal variations were observed in the hydrogen sulfide concentrations in surface sediment pore water. Hydrogen sulfide was detected in summer (<0.1 to 1.6 mg-S L⁻¹) and autumn (<0.1 to 4 mg-S L⁻¹), whereas it was undetectable (<0.1 mg-S L⁻¹) in spring and winter. The slightly higher concentrations of hydrogen sulfide in autumn could be due to the increasing sedimentation flux of POM. Unlike our study, some

earlier studies reported the presence of hydrogen sulfide in all seasons in Hiroshima Bay. Those studies applied AVS extraction methods, which cannot separate different sulfur species and potentially include FeS clusters, iron sulfide nanoparticles, mackinawite, greigite, and pyrite. These different sulfur species might have been present during all seasons and might have resulted in an overestimation of the hydrogen sulfide concentrations.

The different sulfur species present in sediments were identified as sulfate, thiosulfate, elemental sulfur, and pyrite in this study. Thiosulfate was a minor component compared to the other sulfur species. It was concluded that the formation of pyrite and elemental sulfur derived from hydrogen sulfide oxidation played an important role in the scavenging of hydrogen sulfide.

Direct analyses using a combination of detection tubes and XAFS enabled us to reveal spatial distribution of hydrogen sulfide and sulfur species in marine sediments in Hiroshima Bay in greater detail compared to the conventional method of acid volatile sulfide measurement. Our proposed method will be useful to better understand sulfur cycle in terms of identifying sulfur species in marine sediments.

Acknowledgements

This study was partially supported by the Environment Research and Technology Development Fund of the Ministry of the Environment, Japan (S-13) and collaborative research (17AG001; HiSOR, Hiroshima University). The authors would like to thank Dr. Hiroaki Tsutsumi and Tomohiro Komorita, Prefectural University of Kumamoto, for providing the facility for isotope analysis.

References

- Affonso, E.G., Polez, V.L.P., Corrêa, C.F., Mazon, A.F., Araújo, M.R.R., Moraes, G., Rantin, F.T., 2004. Physiological responses to sulfide toxicity by the air-breathing catfish, *Hoplosternum littorale* (Siluriformes, Callichthyidae). Compar. Biochem. Physiol. Part C: Toxicol. Pharmacol. 139, 251-257.
- Aller, R.C, Rude P.D., 1988. Complete oxidation of solid phase sulfides by manganese and bacteria in anoxic marine sediments. Geochim. Cosmochim. Ac. 52, 751-765.
- Archer, D., Emerson, S., Reimers, C, 1989. Dissolution of calcite in deep-sea sediments: pH and O₂, microelectrode results. Geochim. Cosmochim. Ac. 53, 2831-2845.
- Arfaeinia, H., Nabipour, I., Ostovar, A., Asadgol, Z., Abuee, E., Keshtkar, M., Dobaradaran, S., 2016. Assessment of sediment quality based on acid-volatile sulfide and simultaneously extracted metals in heavily industrialized area of

505 Asaluyeh, Persian Gulf: concentrations, spatial distributions, and sediment
 506 bioavailability/toxicity. *Environ. Sci. Pollut. Res.* 23, 9871-9890.

507 Asaoka, S., Yamamoto, T., Takahashi, Y., Yamamoto, H., Kim, K.H., Orimoto, K., 2012a.
 508 Development of an on-site simplified determination method for hydrogen sulfide in
 509 marine sediment pore water using a shipboard ion electrode with consideration of
 510 hydrogen sulfide oxidation rate. *Interdiscipl. Studies Environ. Chem.—Environ.*
 511 *Pollut. Ecotoxicol.* 6, 345-352.

512 Asaoka, S., Hayakawa, S., Kim, K.H., Takeda, K., Katayama, M., Yamamoto, T., 2012b.
 513 Combined adsorption and oxidation mechanisms of hydrogen sulfide on granulated
 514 coal ash. *J. Colloid Interf. Sci.* 377, 284-290.

515 Bostick, B.C., Theissen, K.M., Dunbar, R.B., Vairavamurthy, M.A., 2005. Record of
 516 redox status in laminated sediments from Lake Titicaca: A sulfur K-edge X-ray
 517 absorption near edge structure (XANES) study. *Chem. Geol.* 219, 163-174.

518 Burton, E.D., Bush, R.T., Sullivan, L.A., Hocking, R.K., Mitchell, D.R.G., Johnston, S.G.,
 519 Fitzpatric, R.W., Raven, M., McClure, S., Jang, L.Y., 2009. Iron-monosulfide
 520 oxidation in natural sediments: resolving microbially mediated S transformations
 521 using XANES, electron microscopy, and selective extractions. *Environ. Sci. Technol.*
 522 43, 3128–3134.

523 Caddy, J. F., 2000. Marine catchment basin effects versus impacts of fisheries on semi-
524 enclosed seas . ICES J. Mar. Sci. 57: 628-640.

525 Calmano, W., Mangold, S., Welter, E., 2001. An XAFS investigation of the artefacts
526 caused by sequential extraction analyses of Pb-contaminated soils. Fresenius' J.
527 Anal. Chem. 371, 823-830.

528 Choi, M.M.F., Hawkins, P., 2003. Development of an optical hydrogen sulphide sensor.
529 Sensors and Actuators B 90, 211-215.

530 Cline, J.D., 1969. Spectrophotometric determination of hydrogen sulfide in natural waters.
531 Limnol. Oceanogr. 14, 454-458.

532 Dilling, W., Cypionka, H., 1990. Aerobic respiration in sulfate-reducing bacteria. FEMS
533 Microbiol. Lett. 71, 123-127.

534 Dooley, F.D., Wyllie-Echeverria, S., Roth, M.B., Ward, P.D., 2013. Tolerance and
535 response of *Zostera marina* seedlings to hydrogen sulfide. Aquatic Botany 105, 7-
536 10.

537 Gao, X., Li P., Chen, C.T.A., 2013. Assessment of sediment quality in two important areas
538 of mariculture in the Bohai Sea and the northern Yellow Sea based on acid-volatile
539 sulfide and simultaneously extracted metal results. Mar. Pollut. Bull. 72, 281-288.

540 Gernerden, H., 1993. Microbial mats: A joint venture. Mar. Geol. 113, 3-25.

541 Gray, J.S., Wu, R.S., Or, Y.Y., 2002. Effects of hypoxia and organic enrichment on the
542 coastal marine environment. *Mar. Ecol. Prog. Ser.* 238, 249-279.

543 Habicht, K.S., Canfield, D.E., 1997. Sulfur isotope fractionation during bacterial sulfate
544 reduction in organic-rich sediments. *Geochim. Cosmochimi. Acta* 61, 5351-5361.

545 Hata, Y. , 1960. Relation between the activity of marine sulfate-reducing bacteria and
546 the oxidation–reduction potential of the culture media. *J. the Shimonoseki College*
547 *of Fisheries.* 10, 57-77. (in Japanese with English abstract)

548 Hibino, T., Matsumoto, H., 2006. Distribution of fluid mud layer in Hiroshima Bay and
549 its seasonal variation. *J.Jpn. Soc.Cvil Eng. B*, 62, 348-359. (in Japanese with English
550 Abstract)

551 Hoshika, A., 2008. Sedimentation rates and heavy metal pollution of sediments in the
552 Seto Inland Sea, in: Yabagi, T., (Eds.), *Bottom Environment of Seto Inland Sea.*
553 *Kouseisha Kouseikaku Co., Ltd., Tokyo*, pp. 24-26. (in Japanese)

554 Jalilehvand, F., 2006. Sulfur: not a “silent” element any more. *Chem. Soc. Rev.* 35,
555 1256-1268.

556 Jonge, M.D., Blust, R., Bervoets, L., 2010. The relation between Acid Volatile Sulfides
557 (AVS) and metal accumulation in aquatic invertebrates: Implications of feeding
558 behavior and ecology. *Environ. Pollut.* 158, 1381-1391.

559 Jørgensen, B.B., 1977. The sulfur cycle of a coastal marine sediment (Limfjorden,
 560 Denmark). *Limnol. Oceanogr.* 22, 814-832.

561 Jørgensen, B.B., Revsbech N.P., 1985. Diffusive boundary layers and the oxygen uptake
 562 of sediments and detritus. *Limnol. Oceanogr.* 30, 111-122.

563 Jørgensen, B.B., 1987. Ecology of the sulphur cycle: oxidative pathways in sediments.
 564 In: Cole, J.A., Ferguson, S. (Eds.). *The Nitrogen and Sulphur Cycles*, Cambridge
 565 University Press, Cambridge, pp. 31–63.

566 Jørgensen, B.B., Kasten, S., 2006. Sulfur cycling and methane oxidation, in: Schulz, H.D.,
 567 Zabel, M. (Eds.), *Marine Geochemistry*, 2nd ed. Springer-Verlag, Berlin, pp. 271-
 568 309.

569 Kubáň, V., Dasgupta, P.K., Marx, J.N. , 1992. Nitroprusside and methylene blue methods
 570 for silicone membrane differentiated flow injection determination of sulfide in water
 571 and wastewater. *Anal. Chem.* 64, 36-43.

572 Kuno, A., Matsuo, M., Numako, C. 1999. In situ chemical speciation of iron in estuarine
 573 sediments using XANES spectroscopy with partial least-squares regression. *J.*
 574 *Synchrotron Rad.* 6, 667-669.

575 Lawrence, N.S., Davis, J., Compton, R.G., 2000. Analytical strategies for the detection
 576 of sulfide: a review. *Talanta* 52, 771-784.

- 577 Li, Y.H., Gregory, S., 1974. Diffusion of ions in sea water and in deep-sea sediments.
578 Geochim. Comochim. Acta 38, 703-714.
- 579 Li, W., Sun, W., Yu, X., Du, L., Li, M., 2013. Coumarin-based fluorescent probes for H₂S
580 detection. J. Fluores. 23, 181-186.
- 581 Liamleam, W., Annachhatre, A.P. , 2007. Electron donors for biological sulfate reduction.
582 Biotechnol. Adv. 25, 452-463.
- 583 Lloyd, D., 2006. Hydrogen sulfide: clandestine microbial messenger? Trends in
584 Microbiol. 14, 456-462.
- 585 Machado, W., Villar L.S., Monteiro, F.F, Viana, L.C.A., Santelli R.E., 2010. Relation of
586 acid-volatile sulfides (AVS) with metals in sediments from eutrophicated estuaries:
587 Is it limited by metal-to-AVS ratios? J. Soils and Sediments. 10, 1606-1610.
- 588 McCready, R.G.L., Gould, W.D., Cook, F.D., 1983. Respiratory nitrate reduction by
589 *Desulfovibrio sp.* Arch. Microbiol. 135, 182-185.
- 590 Markovic, S., Paytan, A., Wortmann, U.G., 2015. Pleistocene sediment offloading and
591 the global sulfur cycle. Biogeosci. 12, 3043-3060
- 592 Marumo, K., Yokota, M., 2012. Review on aoshio and biological effects of hydrogen
593 sulfide. Rep. Mar. Ecol. Res. Inst. 15, 23-40. (in Japanese).
- 594 Morse, J.W., Millero, F.J., Cornwell, J.C., Rickard, D., 1987. The chemistry of the

595 hydrogen sulfide and iron sulfide system in natural water. *Earth Sci. Rev.* 24, 1-42.

596 Muyzer, G., Stams, A.J.M., 2008. The ecology and biotechnology of sulphate-reducing

597 bacteria. *Nature Rev. Microbiol.* 6, 441-454.

598 Nriagu, J., Soon, Y.K. 1985. Distribution and isotopic composition of sulfur in lake

599 sediments of northern Ontario. *Geochim. Cosmochim. Acta* 49, 823-834.

600 Otsubo, K., Harashima, A., Miyazaki, T., Yasuoka, Y., Muraoka, K., 1991. Field survey

601 and hydraulic study of “Aoshio” in Tokyo Bay. *Mar. Pollut. Bull.* 23, 51-55.

602 Phillips, D.L., 2012. Converting isotope values to diet composition: the use of mixing

603 models. *J. Mammal.* 93, 342-352.

604 Pjevac, P., Kamyshny Jr, A., Dyksma, S., Mußmann, M., 2014. Microbial consumption

605 of zero-valence sulfur in marine benthic habitats. *Environ. Microbiol.* 16, 3416-3430.

606 Radford, K.J., Cutter, G.A., 1993. Determination of carbonyl sulfide and hydrogen sulfide

607 species in natural waters using specialized collection procedures and gas

608 chromatography with flame photometric detection. *Anal. Chem.* 65, 976-982.

609 Raven, J.A., Scrimgeour, C.M., 1997. The influence of anoxia on plants of saline habitats

610 with special reference to the sulphur cycle. *Annal. Bot.* 79, 79–86.

611 Reese, B.K., Anderson, M.A., Amrhein, C., 2008. Hydrogen sulfide production and

612 volatilization in a polymictic eutrophic saline lake, Salton Sea, California. *Sci.*

613 Total Environ. 406, 205-218.

614 Rice, C.A., Tuttle, M.L., Reynolds, R.L., 1993. The analysis of forms of sulfur in ancient
615 sediments and sedimentary rocks: comments and cautions. Chem. Geol. 107, 83-95.

616 Rickard, D., Luther, G.W. , 2007. Chemistry of iron sulfides. Chem. Rev. 107, 514-562.

617 Rickard, D., Morse, J.W., 2005. Acid volatile sulfide (AVS). Mar. Chem. 97, 141-197.

618 Risgaard-Petersen, N., Revil, A., Meister, P., Nielsen, L.P., 2012. Sulfur, iron-, and
619 calcium cycling associated with natural electric currents running through marine
620 sediment. Geochim. Cosmochim. Acta 92, 1-13.

621 Sakai, S., Nakaya, M., Sampei, Y., Dettman, D.L., Takayasu, K., 2013. Hydrogen sulfide
622 and organic carbon at the sediment–water interface in coastal brackish Lake
623 Nakaumi, SW Japan. Environ. Earth Sci. 68, 1999-2006.

624 Sampei, Y., Matsumoto, E., 2001. C/N ratios in a sediment core from Nakaumi Lagoon,
625 southwest Japan—usefulness as an organic source indicator—. Geochem. J. 35, 189-
626 205.

627 Schippers, A., Jørgensen, B.B., 2002. Biogeochemistry of pyrite and iron sulfide
628 oxidation in marine sediments. Geochim. Cosmochim. Acta 66, 85-92.

629 Schlitzer, R. 2017, <https://odv.awi.de/> (Accessed 16 April 2018)

630 Scholz, F., McManus J., Sommer, S., 2013. The manganese and iron shuttle in a modern

631 euxinic basin and implications for molybdenum cycling at euxinic ocean margins.
 632 Chem. Geol. 355, 56-68.

633 Seiki, T., Date, E., Izawa H., 1991. Decomposition characteristics of particulate organic
 634 matter in Hiroshima Bay. J. Oceanograph. Soc. Japan 47, 207-220.

635 Seiki, T., Date E., Izawa H., 1985. Settling fluxes of suspended particulate matter
 636 estimated from sediment trap catches in Hiroshima Bay. Japan J. Water Pollut. Res.
 637 8, 304-313. (in Japanese with English abstract).

638 Seiki, T., Izawa H., Date, E., Sunahara, H., 1994. Sediment oxygen demand in Hiroshima
 639 Bay. Water Res. 28, 385-393.

640 Simpson, S.L., Ward, D., Strom, D., Jolley, D.F., 2012. Oxidation of acid-volatile sulfide
 641 in surface sediments increases the release and toxicity of copper to the benthic
 642 amphipod *Melita plumulosa*. Chemosphere 88, 953-961.

643 Thamdrup, B., Fossing, H., Jørgensen, B.B., 1994. Manganese, iron, and sulfur cycling
 644 in a coastal marine sediment, Aarhus Bay, Denmark. Geochim. Cosmochim. Acta 58,
 645 5115-5129.

646 Tsujino, M., Arima, S., Kamiyama, T., Uchida, T., 2000. Macrobenthos and meiobenthos
 647 communities is relation to the bottom environment in Kure Bay of Seto Inland Sea.
 648 Bull. Fish. Environ. Inland Sea. 2, 49-56. (in Japanese with English abstract)

649 Wang, F., Chapman, P. M., 1999. Biological implications of sulfide in sediment- A review
650 focusing on sediment toxicity. *Environ. Toxicol. Chem.* 18, 2526-2532.

651 Wei, D., Osseo-Asare, K., 1996. Particulate pyrite formation by the $\text{Fe}^{3+}/\text{HS}^-$ reaction in
652 aqueous solutions: effects of solution composition. *Colloid. Surf. A: Physicochem.*
653 *Engineer. Asp.* 118, 51-61..

654 Whitfield, M. , 1973. A chemical model for the major electrolyte component of seawater
655 based on the Brønsted-Guggenheim hypothesis. *Mar. Chem.* 1, 251-266.

656 Yamamoto, H., Yamamoto T., Takada, T., Mito, S. Takahashi. T. , 2011. Dynamic analysis
657 of oxygen-deficient water mass formed in the northern part of Hiroshima Bay using
658 a pelagic-benthic coupled ecosystem model. *J. Jpn. Soc. Water Environ.* 34,19-28. (in
659 Japanese with English abstract)

660 Yamamoto, T., Ishida, M., Seiki, T., 2002. Long-term variation in phosphorus and
661 nitrogen concentrations in the Ohta River water, Hiroshima, Japan as a major factor
662 causing the change in phytoplankton species composition. *Bull. Japanese Soc. Fish.*
663 *Oceanogr.* 66, 102-109. (in Japanese with English Abstract)

664 Yamamoto, T., Goto, I., Kawaguchi, O., Minagawa, K., Ariyoshi, E., Matsuda O., 2008.
665 Phytoremediation of shallow organically enriched marine sediments using benthic
666 microalgae. *Mar. Pollut. Bull.* 57, 108-115.

667 Yamamoto, T., Kim, K.H., Shirono, K. , 2015. A pilot study on remediation of sediments
 668 enriched by oyster farming wastes using granulated coal ash. Mar. Pollut. Bull. 90,
 669 54-59.

670 Yamamuro, M., Kayanne, H., 1995. Rapid direct determination of organic carbon and
 671 nitrogen in carbonate-bearing sediments with a Yanaco MT-5 CHN analyzer. Limnol.
 672 Oceanogr. 40, 1001-1005.

673 Zhang, J., Guo, W., 2014. A new fluorescent probe for gasotransmitter H₂S:high
 674 sensitivity, excellent selectivity, and a significant fluorescence *off-on* response.
 675 Chem. Comm. 50, 4214-4217.

676 Zhu, Q., Aller, R.C., 2013. Planar fluorescence sensors for two-dimensional
 677 measurements of H₂S distributions and dynamics in sedimentary deposits. Mar.
 678 Chem. 157, 49-58.

679

Figure Captions

Spatial distribution of hydrogen sulfide and sulfur species in coastal marine sediments, Hiroshima Bay, Japan by Asaoka et al.

Fig. 1 Sampling stations in this study

Fig. 2 The spatial distributions of hydrogen sulfide concentration in surface sediments pore water (0-5 cm depth)

Fig. 3 The vertical profiles of the hydrogen sulfide concentration in the core sediment pore water in autumn

Fig. 4 The spatial distributions of sulfur species concentration (mg g^{-1}) in surface sediments

Fig. 5 The concentrations of dissolved of bottom water (1 m above from the seabed)

Fig. 6 Eh of the sediments vs. the concentrations of hydrogen sulfide in the sediment pore water in all samples

Fig. 7 Carbon ($\delta^{13}\text{C}$) and nitrogen ($\delta^{15}\text{N}$) isotope of surface sediments and each endmember

Error bars are standard deviation

Fig. 8 The Eh-pH diagram for the Fe-S-H₂O system

Fig. 9 Corelationship between percent composition of pyrite and sum of sulfate and thiosulfate of sediments

Figures

Spatial distribution of hydrogen sulfide and sulfur species in coastal marine sediments, Hiroshima Bay, Japan by Asaoka et al.

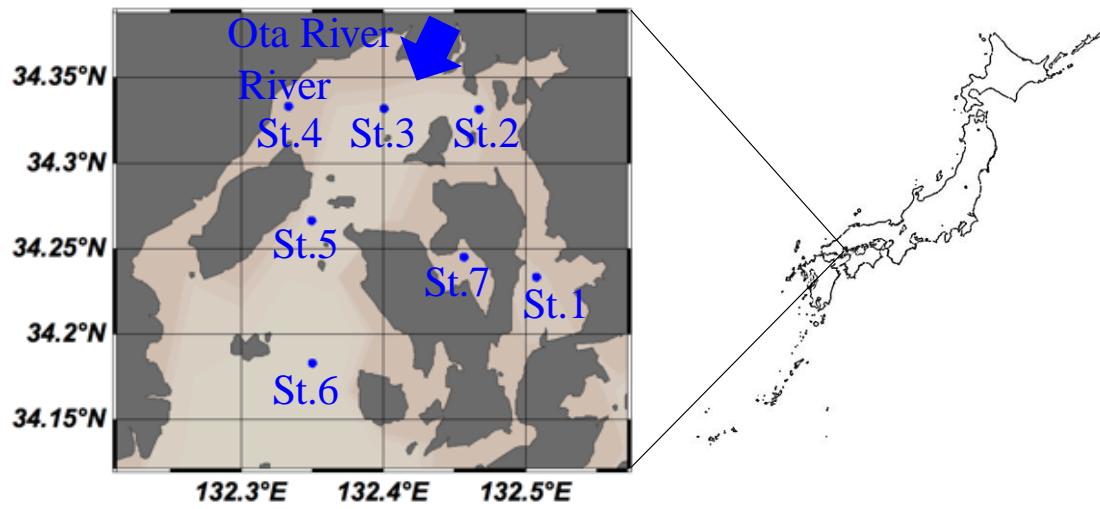


Fig. 1 Sampling stations in this study

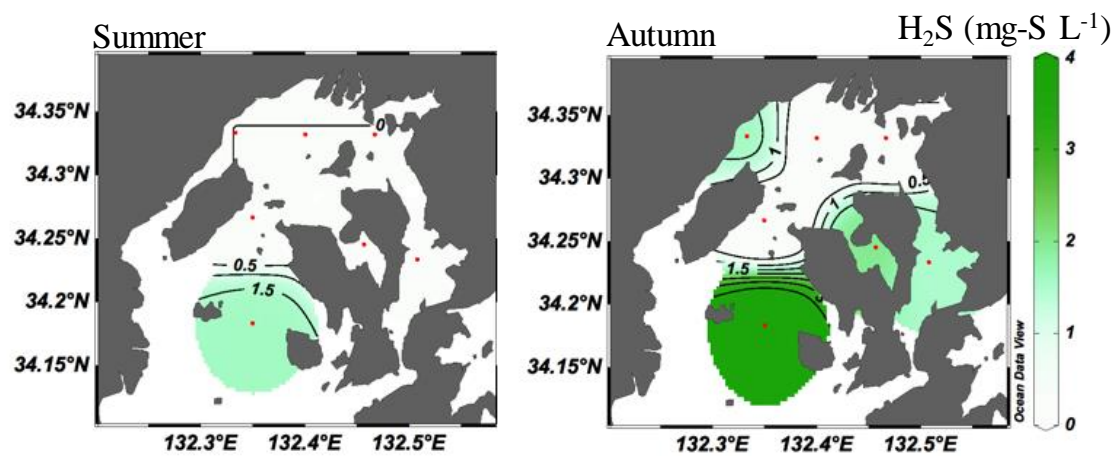


Fig. 2 The spatial distributions of hydrogen sulfide concentration in surface sediments pore water (0-5 cm depth)

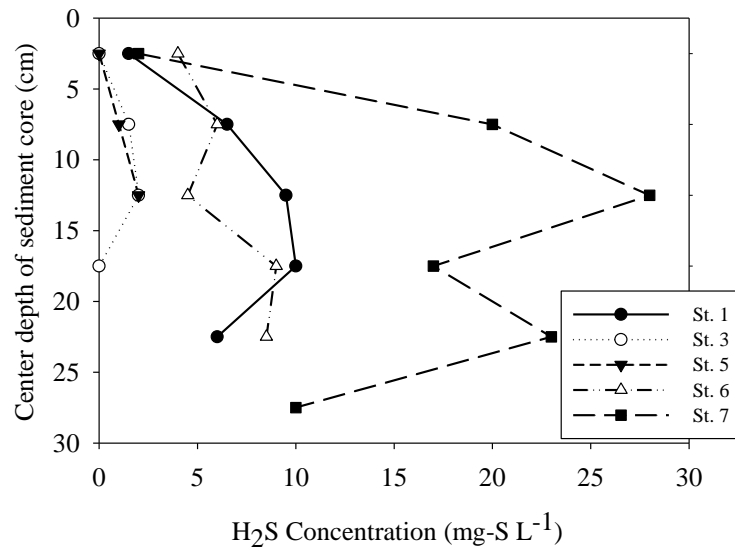


Fig. 3 The vertical profiles of the hydrogen sulfide concentration in the core sediment pore water in autumn

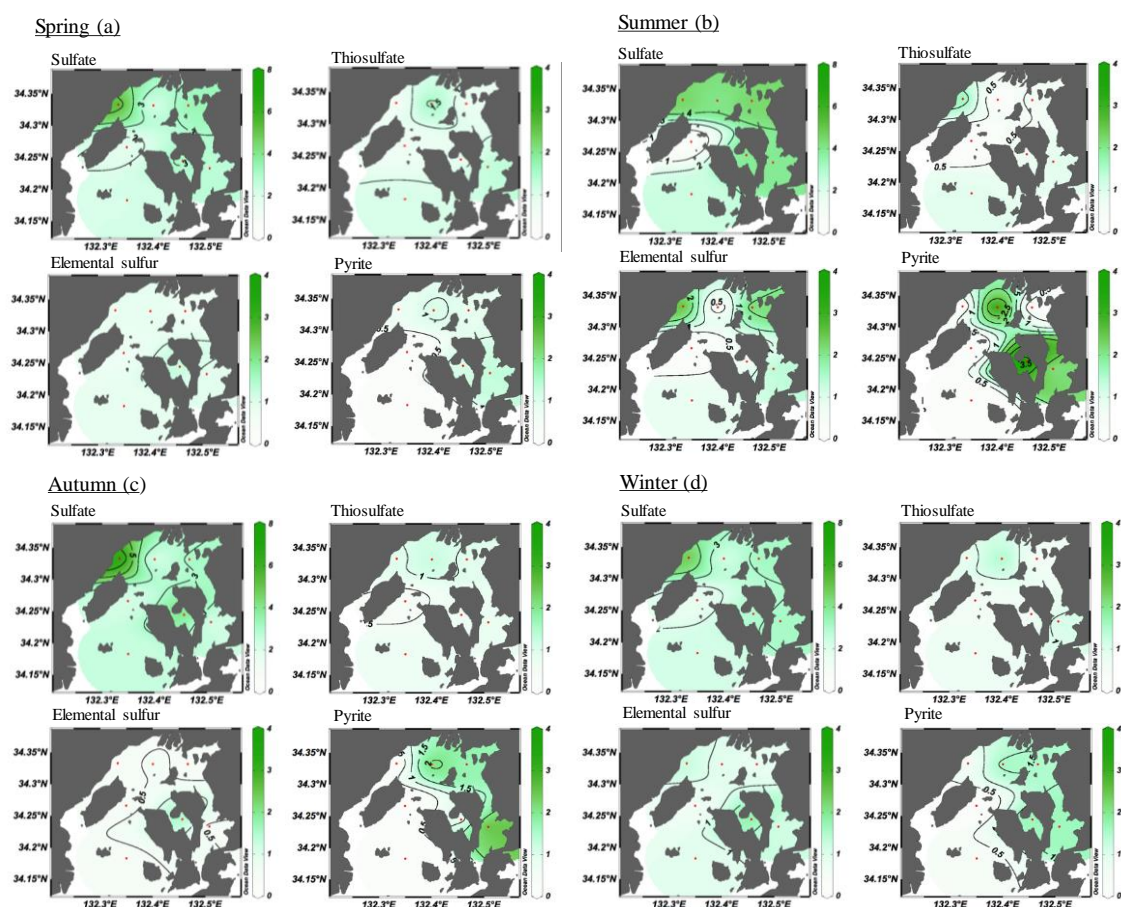


Fig. 4 The spatial distributions of sulfur species concentration (mg g⁻¹) in surface sediments

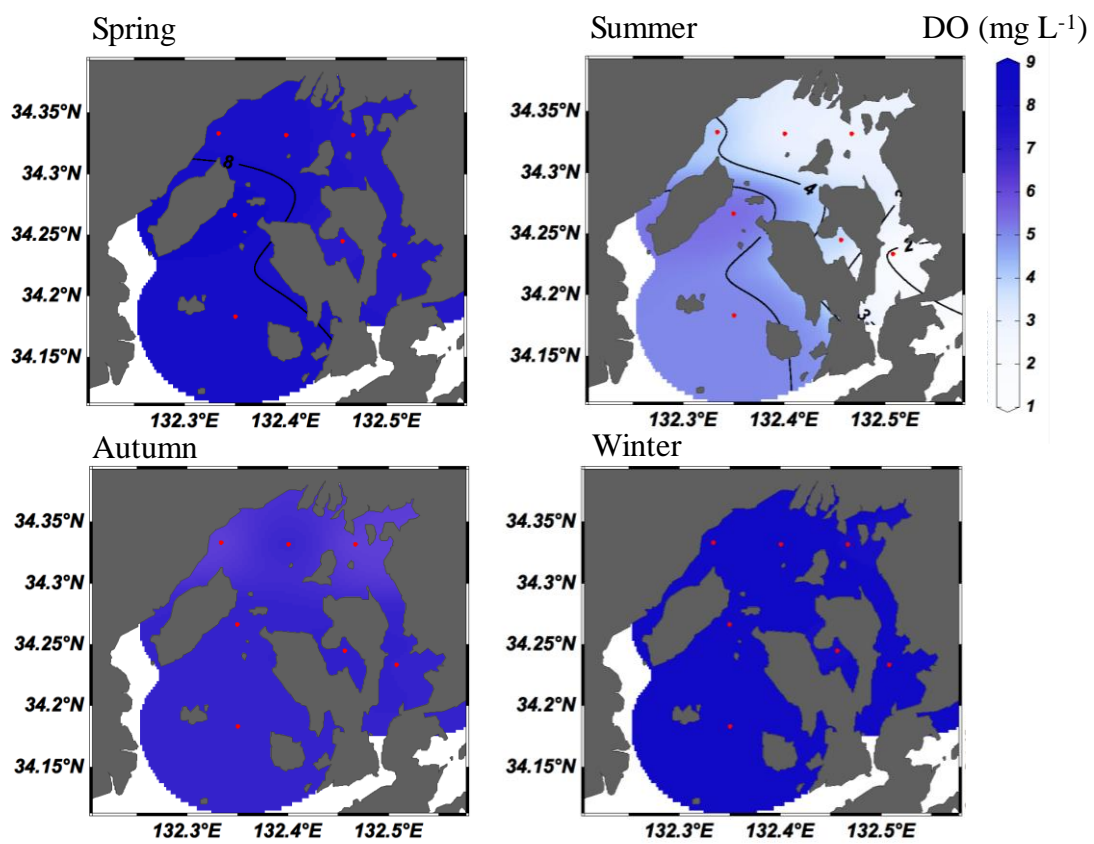


Fig. 5 The concentrations of dissolved of bottom water (1 m above from the seabed)

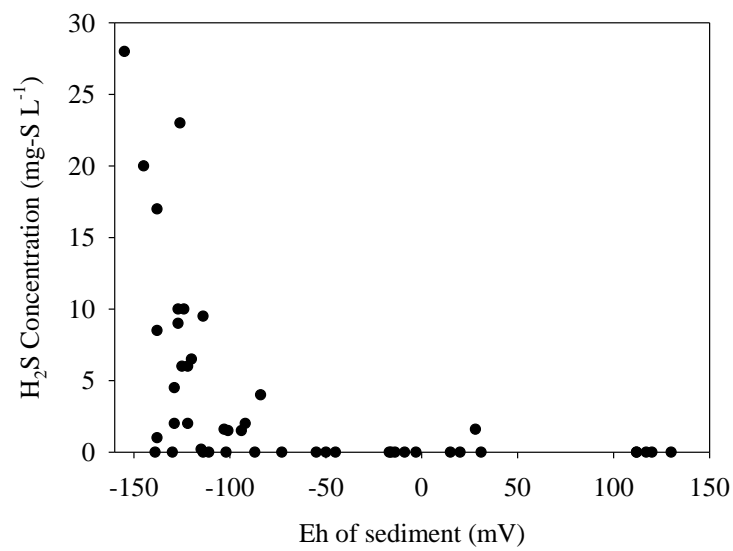


Fig. 6 Eh of the sediments vs. the concentrations of hydrogen sulfide in the sediment pore water in all samples

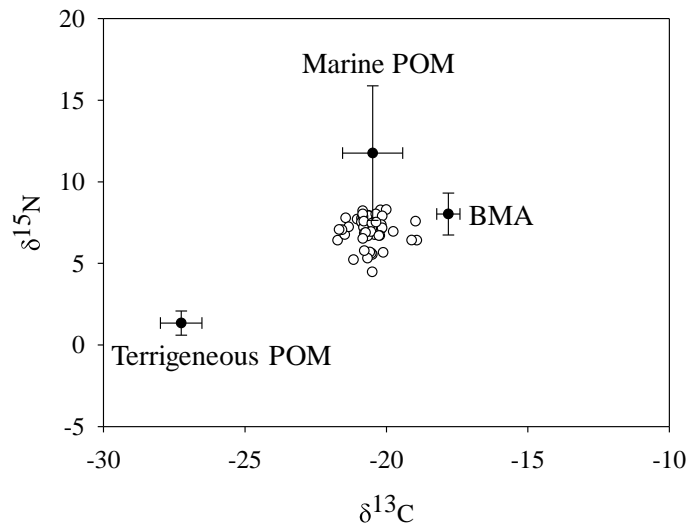


Fig. 7 Carbon ($\delta^{13}\text{C}$) and nitrogen ($\delta^{15}\text{N}$) isotope of surface sediments and each endmember

Error bars are standard deviation

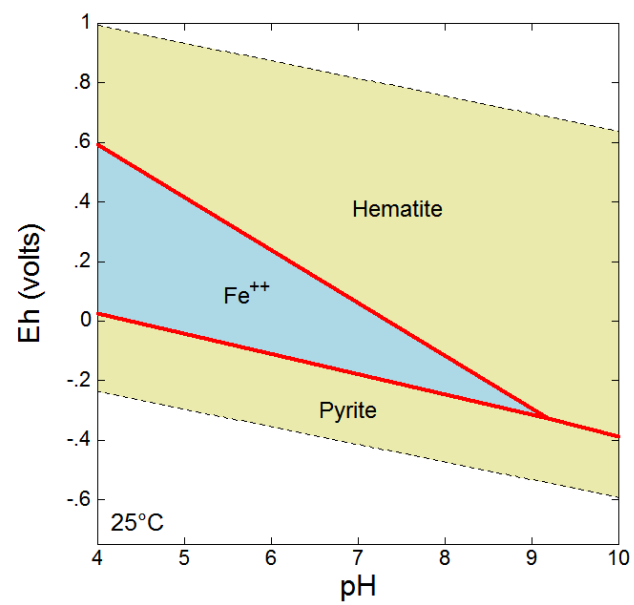


Fig. 8 The Eh-pH diagram for the Fe-S-H₂O system

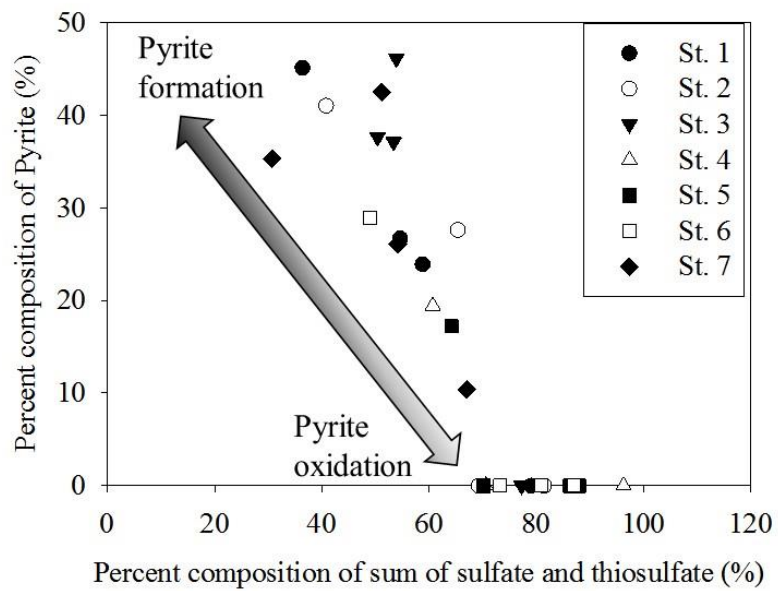


Fig. 9 Corelationship between percent composition of pyrite and sum of sulfate and thiosulfate of sediments

Tables

Spatial distribution of hydrogen sulfide and sulfur species in coastal marine sediments, Hiroshima Bay, Japan by Asaoka et al.

Table 1 Eh and pH of surface sediments

	Spring		Summer		Autumn		Winter	
	Eh (mV)	pH	Eh (mV)	pH	Eh (mV)	pH	Eh (mV)	pH
St. 1	-3	7.9	-111	7.7	-94	7.9	112	8.3
St. 2	112	7.8	15	8.1	-50	7.8	130	8.1
St. 3	-17	7.8	-102	7.8	-87	7.7	117	8.2
St. 4	-16	8.1	-130	7.8	-103	7.8	-9	8.2
St. 5	31	8.1	-139	7.8	-114	7.7	20	8.2
St. 6	-14	8.0	28	7.9	-84	7.8	120	8.4
St. 7	-55	8.6	-115	8.5	-129	7.8	-45	8.0

Table 2 The TOC , TON, C/Norg ratios, LOI, COD and mud content of surface sediments

	TOC (%)	TON (%)	C/Norg	LOI (%)	COD (mg g ⁻¹)	Mud content (%)
St. 1	2.7	0.29	9.1	11	48	74.7
St. 2	2.5	0.29	8.7	12	37	67.4
St. 3	2.5	0.28	9.1	10	40	65.4
St. 4	2.7	0.32	8.5	9.9	42	65.4
St. 5	2.0	0.22	9.2	11	40	10.3
St. 6	2.1	0.23	8.9	11	57	74.3
St. 7	2.2	0.25	8.9	12	49	68.6

The LOI, COD and mud content were obtained from Hibino and Matsumoto, 2006; monitoring data by the Ministry of Land, Infrastructure, Transport and Tourism, Japan

Supplemental materials

Spatial distribution of hydrogen sulfide and sulfur species in coastal marine sediments,
Hiroshima Bay, Japan

Satoshi ASAOKA^{a*}, Akira UMEHARA^b, Sosuke OTANI^c, Naoki FUJII^d, Tetsuji
OKUDA^e, Satoshi NAKAI^f, Wataru NISHIJIMA^b, Koji TAKEUCHI^g, Hiroshi
SHIBATA^g, Waqar Azeem JADOON^a, Shinjiro HAYAKAWA^f

- ^a Research Center for Inland Seas, Kobe University,
5-1-1 Fukaeminami, Higashinada, Kobe, 658-0022 JAPAN
- ^b Environmental Research and Management Center, Hiroshima University,
1-5-3, Kagamiyama, Higashihiroshima, Hiroshima, 739-8513 JAPAN
- ^c Department of Technological Systems, Osaka Prefecture University College of
Technology 26-12, Saiwaicho, Neyagawa, Osaka, 572-8572 JAPAN
- ^d Institute of Lowland and Marine Research, Saga University, 1, Honjyo, Saga, 840-
8502 JAPAN
- ^e Faculty of Science & Technology, Ryukoku University
1-5 Yokotani, Setaooe, Ootsu, Shiga 520-2194, JAPAN
- ^f Graduate School of Engineering, Hiroshima University
1-4-1 Kagamiyama, Higashi-Hiroshima, Hiroshima 739-8527, JAPAN
- ^g National Institute of Technology, Hiroshima College
4272-1, Higashino, Oosakikamishima, Toyota, Hiroshima 725-0231, JAPAN

*Corresponding author:

Tel & Fax: +81-78-431-6357, E-mail: s-asaoka@maritime.kobe-u.ac.jp

Address: Research Center for Inland Seas, Kobe University, 5-1-1 Fukaeminami,
Higashinada, Kobe, 658-0022 JAPAN

Table S1 Sampling stations in this study

St.	Latitude	Longitude	Depth (m)
1	34°-14.0' N	132°-30.5' E	22
2	34°-19.9' N	132°-28.0' E	19
3	34°-20.0' N	132°-24.0' E	15
4	34°-20.0' N	132°-20.0' E	12
5	34°-16.0' N	132°-21.1' E	45
6	34°-11.0' N	132°-21.0' E	36
7	34°-14.7' N	132°-27.4' E	21

Table S2 The spatial distributions of sulfur species concentration (mg g⁻¹) in surface sediments

Spring

St.	Concentration (mg g ⁻¹)					Percent Composition (%)			
	Sulfate	Thiosulfate	Elemental Sulfur	Pyrite	Total Sulfur	Sulfate	Thiosulfate	Elemental Sulfur	Pyrite
1	4.0	0.6	1.6	2.3	8.5	47	7	19	27
2	2.8	0.0	1.2	2.8	6.8	41	0	18	41
3	2.3	1.2	0.9	2.7	7.1	33	18	12	38
4	3.7	1.4	2.2	0.0	7.4	51	20	29	0
5	1.2	0.3	0.4	0.4	2.4	52	12	19	17
6	2.3	0.0	1.0	1.3	4.6	49	0	22	29
7	2.5	0.0	2.8	2.9	8.1	31	0	34	35

Summer

St.	Concentration (mg g ⁻¹)					Percent Composition (%)			
	Sulfate	Thiosulfate	Elemental Sulfur	Pyrite	Total Sulfur	Sulfate	Thiosulfate	Elemental Sulfur	Pyrite
1	4.0	1.0	1.4	2.0	8.4	47	12	17	24
2	4.5	0.6	2.3	0.0	7.4	61	8	31	0
3	4.0	0.0	0.0	3.4	7.5	54	0	0	46
4	4.6	1.8	2.7	0.0	9.0	51	20	29	0
5	0.5	0.1	0.1	0.0	0.7	77	11	12	0
6	2.4	0.9	0.8	0.0	4.2	59	22	19	0
7	3.9	0.7	0.6	3.8	8.9	44	7	6	43

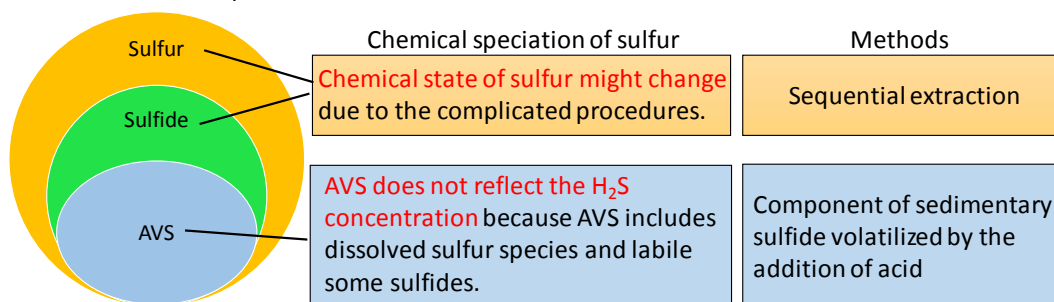
Autumn

St.	Concentration (mg g ⁻¹)					Percent Composition (%)			
	Sulfate	Thiosulfate	Elemental Sulfur	Pyrite	Total Sulfur	Sulfate	Thiosulfate	Elemental Sulfur	Pyrite
1	2.2	0.8	0.3	2.7	5.9	36	13	6	45
2	3.1	0.9	0.4	1.7	6.2	51	15	7	28
3	1.9	1.3	0.6	2.2	6.1	32	21	10	37
4	6.9	0.9	0.3	0.0	8.1	85	11	4	0
5	2.2	0.4	0.4	0.0	3.1	73	13	14	0
6	2.5	0.7	0.5	0.0	3.7	69	18	13	0
7	4.1	0.7	1.6	0.7	7.1	58	9	23	10

Winter

St.	Concentration (mg g ⁻¹)					Percent Composition (%)			
	Sulfate	Thiosulfate	Elemental Sulfur	Pyrite	Total Sulfur	Sulfate	Thiosulfate	Elemental Sulfur	Pyrite
1	3.3	2.0	1.4	0.0	6.7	49	30	21	0
2	3.8	0.5	1.0	0.0	5.3	72	9	19	0
3	2.1	2.1	1.2	0.0	5.4	38	39	23	0
4	4.1	0.0	1.3	1.3	6.7	61	0	20	19
5	1.4	0.9	1.0	0.0	3.4	42	28	30	0
6	1.8	1.4	1.2	0.0	4.5	42	33	27	0
7	2.1	0.9	1.1	1.4	5.5	38	17	20	26

Problems with the previous studies



This study

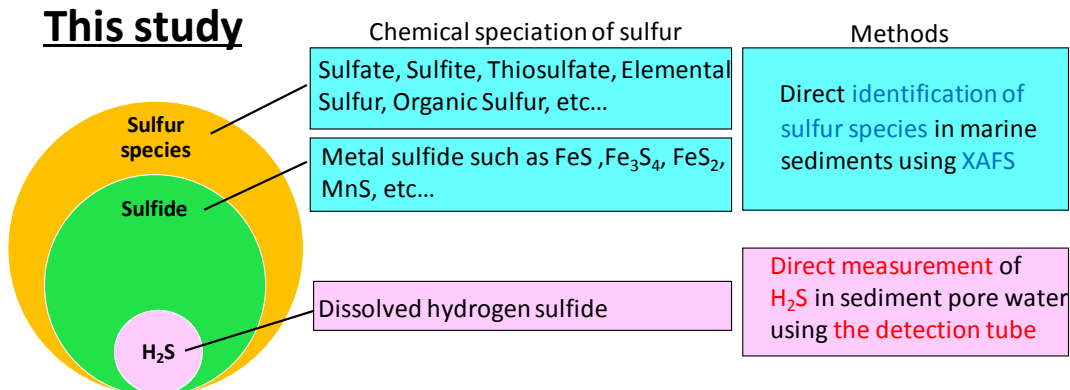


Fig. S1 Description on this study

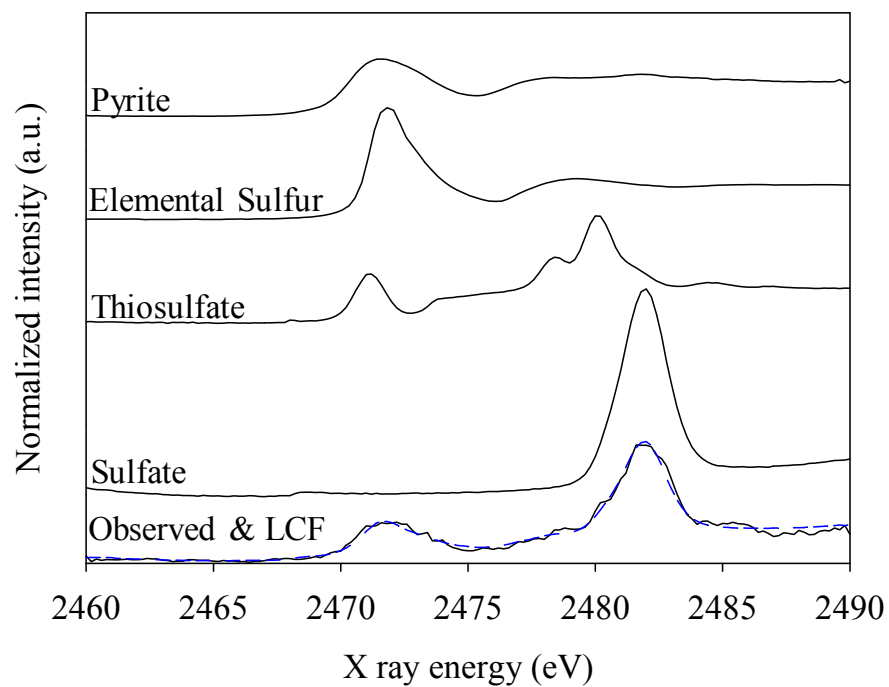


Fig. S2 The Sulfur K edge XANES spectra and the linear combination fit (LCF) of sulfur species of surface sediments (0-5 cm layer) in spring at St. 1.
Blue dotted line is LCF by 4 sulfur standard.

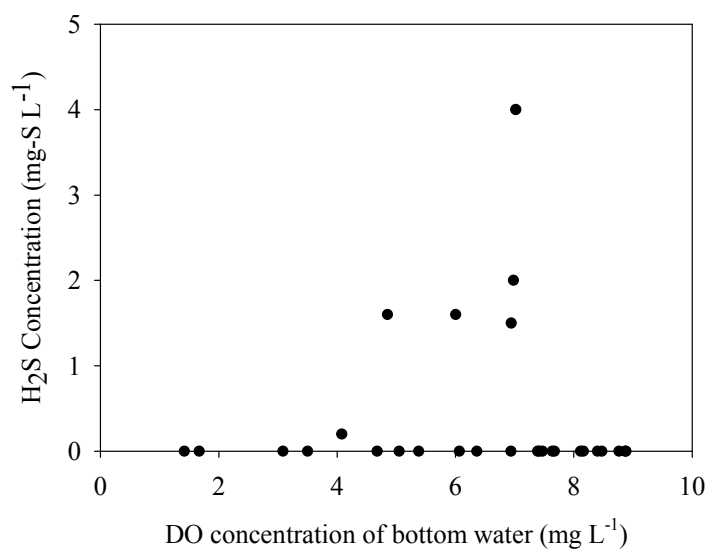


Fig. S3 Dissolved oxygen concentration of bottom water vs. concentration of hydrogen sulfide in sediment pore water in all samples

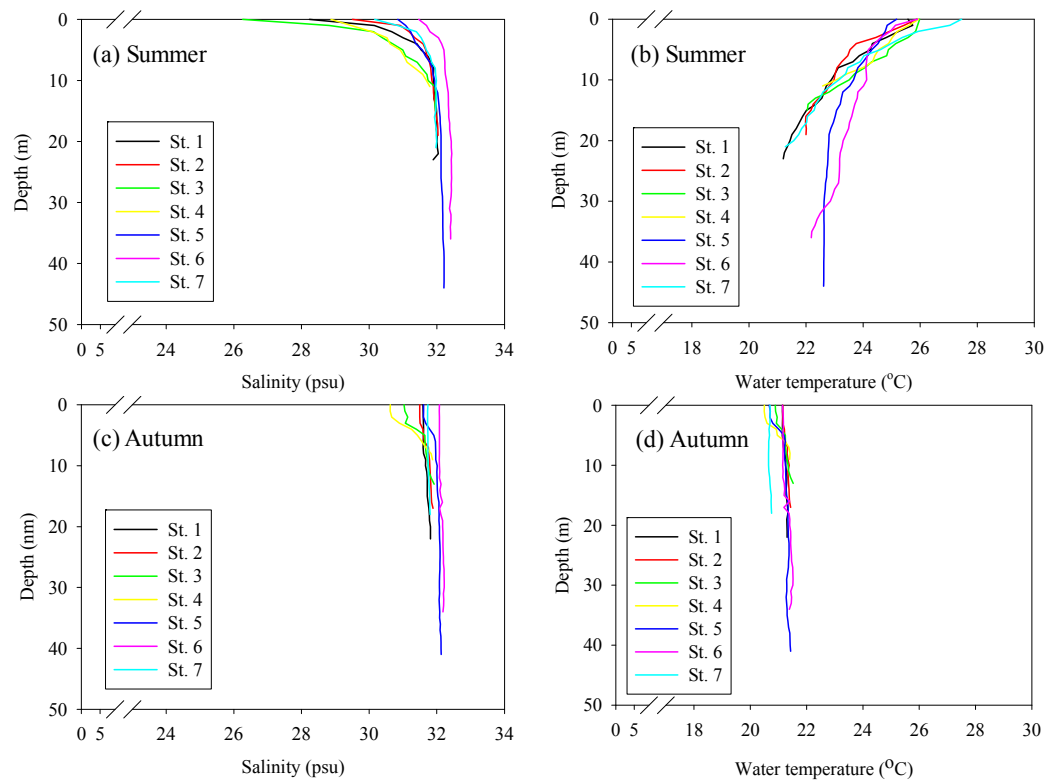


Fig. S4 The vertical profiles of salinity and water temperature in summer and autumn

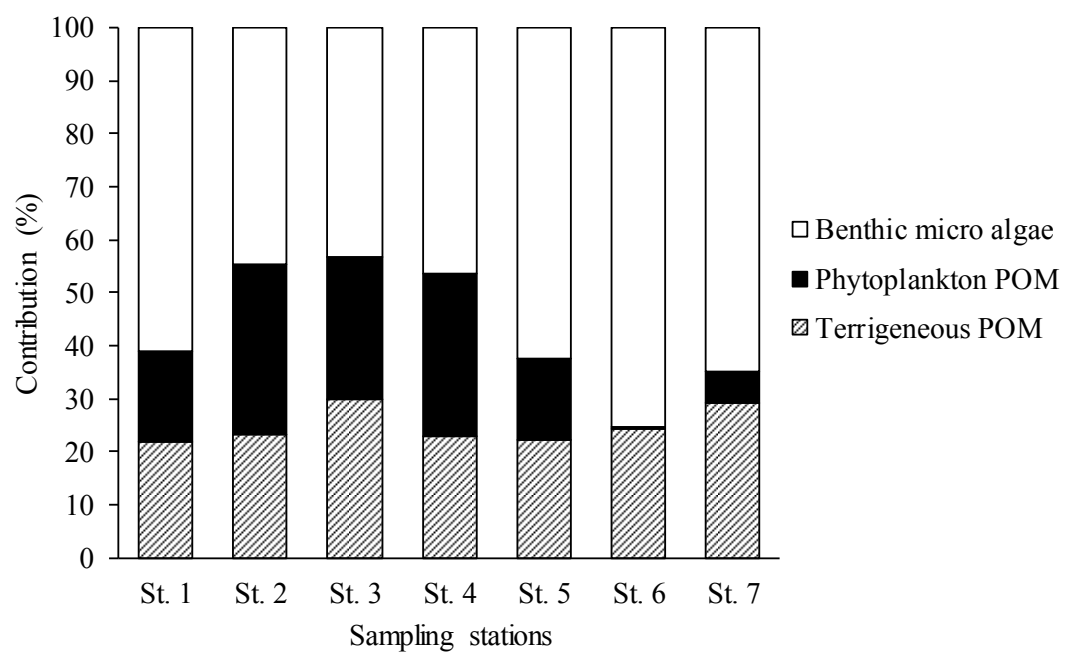


Fig. S5 The annual average of contribution of organic matter in the sediments derived from each source.